Development of a Novel Compression-Based Piezoelectric Traffic Model for Improving the Roadways Energy Harvesting System by Applying the Celular Atomata Traffic Model

Saleh Gareh*‡, B. C. Kok*, M.H. Yee**, Abdoulhdi. A. Borhana ***, S. K. Alswed*
(salehgareh@gmail.com, bckok@uthm.edu.my, mhyee@uthm.edu.my, amhmad@uniten.edu.my, sageralswed@gmail.com)
*Department of Electrical Power Engineering, Faculty of Electrical & Electronic Engineering, UTHM 86400, Johor, Malaysia.
**Faculty of Technical and Vocational Education, Universiti Tun Hussein Onn Malaysia.
***Department of Mechanical Engineering, College of Engineering, Universiti Tenaga Nasional, 43000 Kajang, Selangor Darul Ehsan.

‡ Corresponding Author; Saleh Gareh, Department of Electrical Power Engineering, Faculty of Electrical & Electronic Engineering, UTHM 86400, Johor, Malaysia, salehgareh@gmail.com
Received: 14.08.2019 Accepted:17.09.2019

Abstract- The purpose of this paper is to conduct simulations to increase and analyse the harvested energy in roadway applications. An electromechanical-traffic model of compression-based piezoelectric energy harvesting that exploits the vibrations derived from traffic movement is simulated. The model also being studied on the critical system parameters (e.g. behaviour of traffic flow, number of vehicles, the optimum electrical load, the maximum voltage and the area) accurately based on the simulation of data. Therefore, these factors are considered when designing the traffic model to produce the optimal power. The most significant outcome of this research is the harvesting of electrical energy from piezoelectric arrays by using roadway applications to generate various scales of useable power. The focus from vehicles are on testing and simulating one set array of Piezoelectric Cymbal Transducer (PCTs) and two set arrays of PCTs. By proposing the model, simulating it under different parameters include mean arrival rate (λ), resistance, single lane, two lanes, single PCT and arrays of PCTs. Besides, the Cellular Automata (CA) traffic model is used to represent the traffic flow model. On average, the obtained results show that the highest total power is generated at the highest arrival rate and low resistance. The generated power for a single lane with 2 arrays of PCTs is as much as 170 W and 345 W for two lanes with two arrays of PCTs. The results also show that at low resistance the output power increases whenever the number of PCTs and lanes increase.

Keywords Piezoelectric Energy Harvester; Mean Arrival Rate (λ); two-degree-of-freedom model (2DOF); Cellular Automata (CA); Piezoelectric Cymbal Transducer (PCT) harvester.

1. Introduction

The energy scavenging and energy harvesting techniques are described as the applications which capture, exploit or implement the unused or depleted energy, thereby converting it to a usable form. In this process, energy is extracted from an ambient environment and converted to consumable electric energy. Power energy harvesting that are exploited are of different types, like mechanical energy, vibration, wind, sunlight, strain and kinetic energy. Recently, thermal and vibration-based energy sources have garnered a lot of popularity and are being harvested as they generate a lot of energy, which could help in solving the global energy issues, without depleting the natural energy resources. Figure 1 presents the easiest process used for harvesting energy. Initially, the energy was captured and stored, before being used [1].

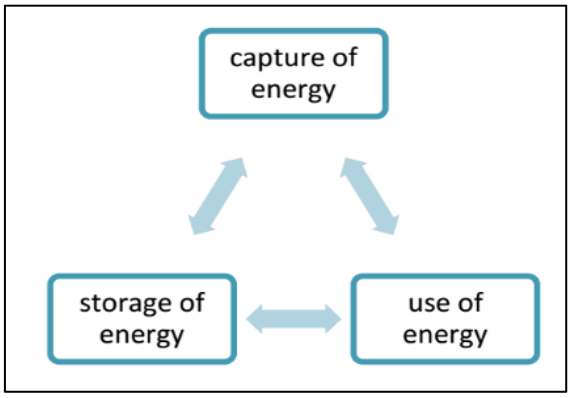

Fig 1. Simple Energy Harvesting Procedure

The piezoelectric materials are ideally used for harvesting energy from the vibrations existing in the environment, as they consist of a basic structure which can effectively convert the mechanical strain into electrical charge without utilising any extra power [2]. Thereafter, the power is again extracted from the piezoelectric materials with the help of a micro-scale energy harvesting system which is used in sensors and smaller

electronic devices. The roadway energy harvester is regarded as a low frequency application which generates energy under a suitable compression force. In addition, the pressure is usually loaded in a vertical direction from the traffic so that the compression piezo can withstand this pressure. The roadway energy harvester generates power as a pulse that is registered with each compression cycle. The most popular harvester system is a cantilevered beam with piezoceramic Lead Zirconate Titanate (PZT) layers, which is used for high frequency sensor applications as it is easier to obtain the resonance frequency with such a mechanism, unlike the less popular compression ceramic system. However, very few researches are available regarding the harvesting of energy from traffic through the development of stacked configuration-based piezoelectric harvesters. As such, this study investigated the connection between a traffic model and a compressed piezo model. The differences between cantilever and compression structures are illustrated in Figure 2 [3].

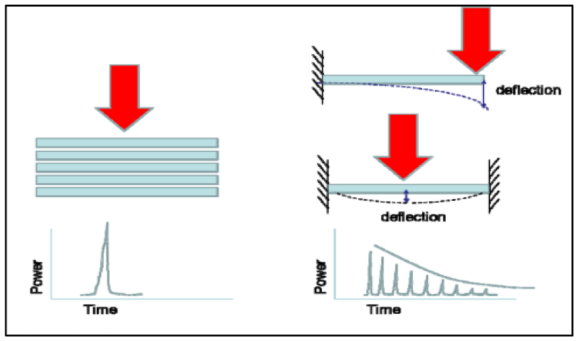

Fig 2. Different performance characteristics noted in the compression-based and cantilever energy harvesters [4]

Many properties must be considered while characterising the energy sources like high voltage, current and power density; physical properties like shape, size and weight; environmental properties like water resistance and operating temperature range; along with the maintenance and operational properties. The authors [5, 6] have summarised a few energy harvesting techniques and described their power density, as described in Table 1. After investigating the studies related to the energy harvesting sources described in the above table, the researchers concluded that solar energy showed the maximal power density, when outdoors, however, it showed a lower energy density, when indoors. On the other hand, vibration energy harvesting showed a relatively high-power density in comparison to other sources. Additionally, vibrational sources were ubiquitous and are present in many locations like roads, air ducts, and building structures [7-10].

Table 1. A summary of the common energy harvesting techniques and their power densities

Energy Harvesting Sources	Power density	Reference(s)
Solar	Outdoor: 15000 μW/cm^3 Indoor: 10 μW/cm^3	[11]
Vibration	Electrostatic: 50 ~ 100 μW/cm^3	[12] [13]
	Electromagnetic: 119 nW/mm^3	[14]
	Piezoelectric: 250 μW/cm^3	[15]
Thermal	40 ~ 60 119 μW/mm^2 (5°C gradient)	[16]

1.1 Piezoelectricity

In Greek, 'Piezo' refers to pressure, while piezoelectricity can be translated to "electricity by pressure". Furthermore, piezoelectricity integrates the electrical and mechanical features of a few materials. The materials which displayed a piezoelectric effect are called the piezoelectric materials. In general, the piezoelectric effect can be classified into direct and converse effects. Thus, after compressing (or mechanical straining) the piezoelectric materials, an electric charge is accumulated at the electrodes, which are positioned at the surface. This refers to a direct piezoelectric effect (or piezoelectric transducer). In Figure 3a, the researchers have described a simple piezoelectric transducer, while Figures. 3b and c present the longitudinal and transverse generators, respectively [17].

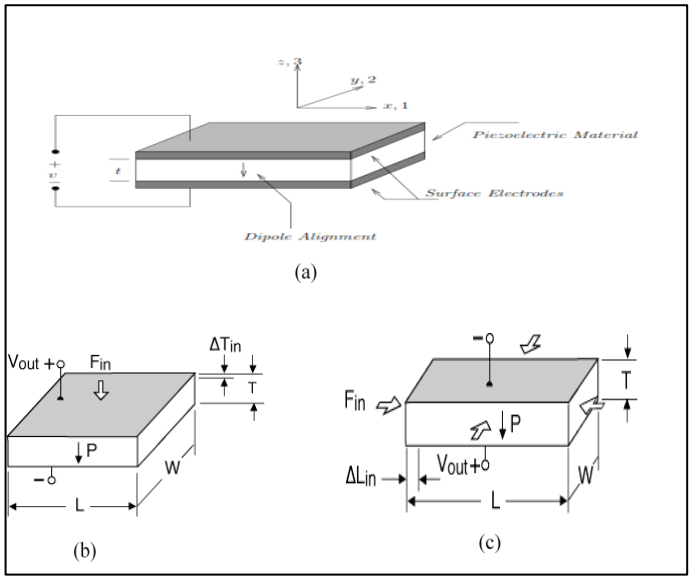

Fig 3. Basic piezoelectric transducer (a) Schematic illustration of a piezoelectric transducer (b) Longitudinal (d33) (c) Transverse (d31) [18]

1.2 Earlier investigations on piezoelectric energy harvesting

Many techniques were suggested for extending the energy harvesting process for a broad frequency bandwidth [19]. For example, mechanical stress was applied to the converter to tune its resonance frequency. The conversion of the vibration energy into electrical energy was initially proposed by Williams and Yates [20]. They determined 3 possible vibration-to-electric energy conversion techniques, i.e., electromagnetic, electrostatic and piezoelectric transductions. Also, [21] modelled the piezoelectric energy harvesting techniques from the pavement deformation that occurred due to vehicular movements. In the case of smooth-moving traffic conditions (i.e., v = 30 m/s), the immediate power output was seen to be maximal at 41.2 and 47.26 mW for the single-wheel and four-wheel loads, respectively.

In the civil constructions portray a basic vibration frequency of less than 10 Hz can be noted [22]. Accordingly, traffic applications in this area are deemed low frequency applications. A separate effort by [23] highlighted the harvesting of energy from vibrations emanating from the

movement of traffic over bridges. This was achieved with the utilization of a cantilever piezoelectric harvester. The researchers noted that an average amount of power of 0.03 mW could be generated in the region, with the regulated voltage ranging between 1.8 and 3.6 V, at a frequency less than 15 Hz. [24] first developed the MEMS-based micro scale power generator device. Furthermore, the design of the 170 μm × 260 μm PZT cantilever device involved a flat configuration and included the proof mass at the end. This beam successfully generated 1 μW of uninterrupted electrical power, at 2.4 V dc for the 5.2 MΩ resistive load. Additionally, Hard and soft PZT ceramic samples acquired from American Piezoceramics incorporated were utilized for the harvesting of energy under elevated force (∼100 N) at a frequency of (∼100–200 Hz). At a frequency of 100Hz and a force level of 70N, 52 mW power was realized from a cymbal measured across a 400 kΩ resistor. The investigation opted for cymbal transducers instead of other transducers such as multilayer stacks and bimorphs as cymbal transducers come with higher piezoelectric charge coefficients (d^{eff}) and piezoelectric voltage coefficients (g^{eff}) [25] and [24] observed that cantilever-based piezoelectric devices are mainly directed towards applications in the vein of microelectromechanical systems (MEMS). A further investigation by [26] where they studied a Piezoelectric Cymbal Transducer (PCT) to identify its capacity for harvesting in a mechanical as well as electrical setting. An overall power production of 0.46 mW was realized with a PCT measuring 32mm in width together with a 0.3mm thick end under a 50N force across a 3MΩ load resistance. Of late, this design (as displayed in Figure 4) has been employed in a range of applications that include actuators [27-30]. This device was able to generate a maximal output power of ≈1.2 mW at the vehicle load frequency of 20 Hz. This was beneficial for the roadway applications since this technique included the compression-based piezoceramic technology and supported the low-frequency excitation. A Piezoelectric Cymbal Transducer (PCT) was an off-resonance energy harvester, with the piezoelectric stack configuration. The researchers used the cymbal structure for improving the output of energy harvesters.

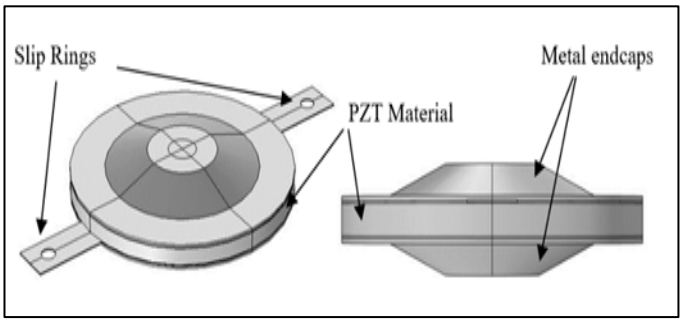

Fig 4. Structure of the Piezoelectric Cymbal Transducer Transducer [26]

Table 2 compared 3 research groups, who applied the piezoelectric technology for generating energy from the roadways. The report showed that higher power was generated using one lane compared to others.

Table 2. Comparison of 3 research groups who used the piezoelectric technology for generating energy from roadways

Parameter	Genziko	ODOT	Innowattech
Generated Power Per Km (single Lane)	13-51 KW	486 KW	100-200 KW
Vehicles per Hour (single Lane)	600-2250	600	600

In our previous paper a single PCT was tested, the produced power was about 14.126 W, 29.746 W and 6.47 W in a single-lane traffic model with different arrival rates λ. This amount of power could be sufficient, in case of planting arrays of the proposed PCTs along the road.

There are several studies discussed and experimented energy harvesting [31, 32]. Some of them focused on nonrenewable energy sources whereas others focused on renewable energy sources [33-38]. Many renewable energy harvesting sources generate renewable energy like the thermoelectric generators, photovoltaic cells, wind turbine and mechanical vibration appliances like the piezoelectric and even the electromagnetic mechanisms. The investigation proves that, vibration as energy harvesting source provided high power density compared to the other sources. Although there are several studies focused on harvesting power based on vibration, still this area has issues can be addressed include not limited to; improve the energy harvested and increase the power density as that important to operate sensors or other small electronic devices. In addition, most existing methods studied and investigated different method of harvesting power from different vibration source without considering and focusing on different parameters such as testing several mean arrival raters, different resistance, several road lanes, and they mostly ignored testing and simulating one set array of 4*4 PCTs and two set of 4*4 arrays of PCTs. Therefore, it is a paramount to study and investigate power based on vibration to attempting energy harvesting improvement and to attempt to increase the power density as that important to operate sensors or other small electronic devices as well as to study and investigate different vibration source considering and focusing on different parameters such as testing several mean arrival raters, different resistance, several road lanes, and they mostly ignored testing and simulating one set array of 4*4 PCRs and two set of 4*4 arrays of PCTs. In this paper, an electromechanical-traffic model of compression-based piezoelectric energy harvesting that exploits vibrations derived from traffic movement is tested and simulated to harvest energy from this movements.

2. Methodology

Here, the model taxonomy can be categorised in 2 categories, as described in Figure 5. The piezoelectric model was used, based on an electromechanical piezoelectric 2DOF, similar to that described earlier [29, 39-41]. The electromechanical piezoelectric model was used for lab experiments to test the prototype under harmonic excitations. While using the model for determining the general traffic

pattern, the researchers need to stimulate the complete electromechanical-traffic model for understanding the actual picture. The traffic model was developed using the Cellular Automata (CA) model and could be initialised in the single-lane or the multiple-lane models [42].

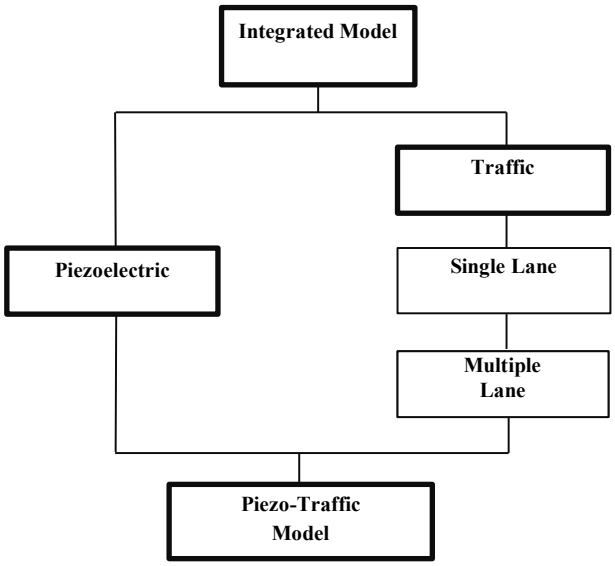

Fig 5. Taxonomy of Models

The researchers proposed the use of a compression-based piezoelectric model as the roadway energy harvester. Under dynamic compression forces, each compression cycle generated energy as pulses [39]. The proposed model compression based piezoelectric traffic model (CPTM) requires a collaboration of three models to be effective in modelling a real-life scenario of a compression based energy harvesting system. The models involved are the traffic model, vehicle dynamics model and piezoelectric model as shown in figure 6. The traffic model enables the simulation of traffic on the road. This provides the set of vehicles that interact with the piezoelectric model to generate the voltage and power to the energy harvesting system. The vehicle dynamics model connects the traffic model and the piezoelectric model such that the movement of vehicle from the former is properly reflected.

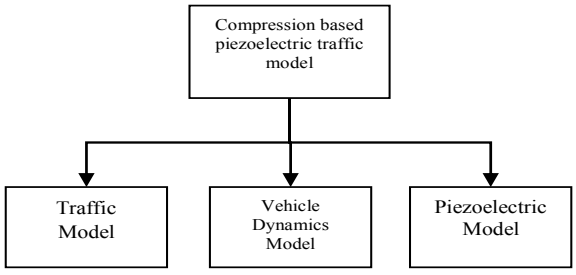

Fig 6. Involved models to simulate real-life scenario of a compression based energy harvesting system.

2.1 2DOF Piezoelectric model

It was noted that the traffic model interacted with the piezoelectric model. It has been recommended that the external intervention stimulated the attainment of optimal frequency. Hence, this model was used for determining the optimal solution for energy harvesting.

The piezoelectric model that was selected for this simulation was a 2-Degree-Of-Freedom (2DOF) model, developed by [39]. This model could be used for civil buildings, highways and roads for harvesting electrical energy. It displayed many mechanical and electrical properties. Figures 6(a) and 6(b) describe the PCT and electromechanical models. The PCT produces electric charge and converts the external kinetic energy into electrical energy [43].

The researchers used PCT for enduring the large compressive loads existing in the civil infrastructure system applications. This model can be effectively embedded into roads, civil buildings and highways for harvesting electric energy. They expected the piezoelectric cymbal to generate an electrical charge by converting kinetic energy into electrical energy.

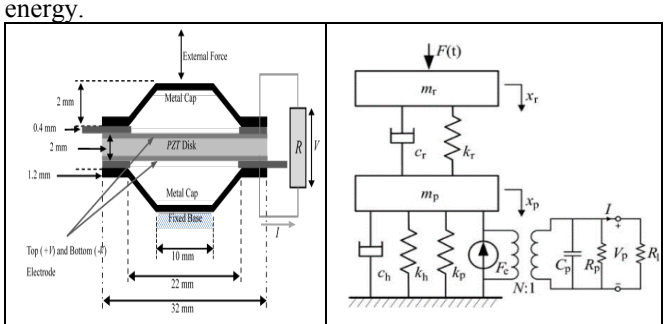

(a) (b)

Fig 7. (a) Piezoelectric Cymbal Transducer (PCT) [44] and (b) Electrical and mechanical properties of piezoelectric model [40].

Table 3 describes the general properties of the piezoelectric material selected in the study and compares it to the standard properties of piezoceramic materials stated by the APC International.

Table 3. Properties of the piezoelectric materials [45]

Property	APC 840	APC 855	APC 880
$d_{33}[pm/V]$	290	630	215
κ_{33}	0.72	0.76	0.62
$\varepsilon_{33}^{T}/\varepsilon_0$	1000	3800	1800
Q_m	500	65	1000

The researchers developed the electromechanical-traffic model using a single PCT which consisted of the poled piezoelectric disk (which was covered with the electrodes on their bottom and top surfaces). Table 4 presents the parameters used in the piezoelectric model.

Table 4. Properties of the piezoelectric materials selected in the study

Parameter	Symbo	Value
mass of metal cap layer	mr	0.0330
damping of metal cap layer	cr	0.0300
elastic coefficient of metal cap	kr	570000
deformation of metal cap layer	xr	0.1000
mass of piezoelectric material	mp	0.1220
elastic coefficient of	kp	270000000
Damping of mechanical structure	ch	5.1000
elastic coefficient of mechanical	kh	275000000

electromechanical conversion	N	0.7600
Capacitor	Cp	0.00000007

2.2 Traffic Model

Different studies used a variety of traffic models. In this report, the researchers have investigated the traffic model, described earlier [46], which used the cellular automata [47] mechanism for modelling the complex behaviour of the traffic based on a discrete timeline. This traffic model was developed for simulating the general vehicular movement over the piezoelectric harvester. Figure. 8 shows a diagram of the car that was speeding with 'a' acceleration. This traffic model could estimate the car's velocity (v) if it could estimate the vertical forces (Fz) of the front (F_{Z1}) and rear tires (F_{Z2}) with those on the road [48]. For this purpose, the values related to the mass of the car (m), wheelbase (l), gravity constant (g), distance measured between the Centre Of the Gravity (COG) and the front tire (a_1), rear tire (a_2) and the ground (h), and the acceleration (a) of the car were required.

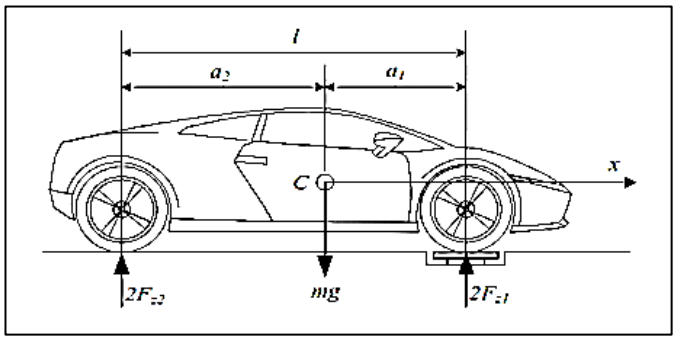

Fig 8. Simple Example for the Traffic Model [48]

It was noted that forces differed for the front (F_{z1}) and back tires (F_{z2}) because of the vehicular dimensions, which affected the centre of gravity. Equations. 1 and 2 present the forces affecting the front and the rear tires:

$$F_{z1} = \frac{1}{2}mg\frac{a_2}{l} - \frac{1}{2}mg\frac{h}{l}\frac{a}{g} \quad (1)$$

$$F_{z2} = \frac{1}{2}mg\frac{a_1}{l} + \frac{1}{2}mg\frac{h}{l}\frac{a}{g} \quad (2)$$

Wherein, *a*- acceleration of the vehicle; F_{z1}- normal forces acting on the front wheels; F_{z2}-normal forces acting on the rear wheels; l- wheelbase; *m*- mass of the car; a_1- distance between the centre of mass and first axle; a_2- distance between the 2nd axle and the centre of mass; *C*- centre of mass of the vehicle; *h*- height of *C*; *g*- acceleration of gravity.

2.3 Integration of the Vehicular Dynamic Model; Traffic Model and the Piezoelectric Model

In the study, the researchers proposed the (CPTM) was based on the integration of 3 different models, i.e., the vehicle dynamic model; traffic model and the piezoelectric model. Figure 9 showed that the traffic model initially received the arrival rate, which was described as the traffic flow. Thereafter, velocity (v) of every vehicle which activated the piezoelectric device was assessed. Thereafter, the vehicle dynamic model used the velocity (v) of the vehicle for calculating the frequency (f) and the vertical force (F). Lastly, the piezoelectric model used the estimated values of power (W) and voltage (V).

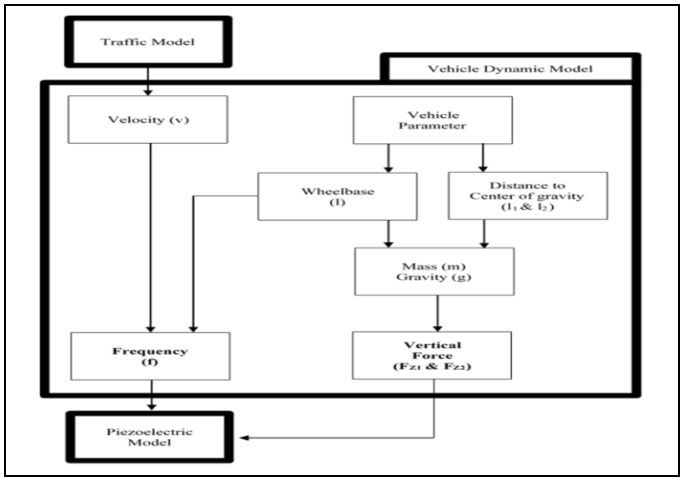

Fig 9. Integration of the Vehicular Dynamic Model; Traffic Model and the Piezoelectric Model

2.4 Cellular Automata

The Cellular Automata (CA) had a flexible structure which consisted of cells wherein every cell evolved through a group of states which was controlled by some rules. In this case, the road is partitioned into a constant length Δx while the time is separated into stages of Δt. Figure 10 shows simple cellular automata of three cells that oscillated randomly between two states, either black or white after each second. If the middle cell is white and there are two black cells on both sides, then the cellular automata would pause for two seconds before continuing. The behaviour of cells through the Time, T1-T6, describes the CA.

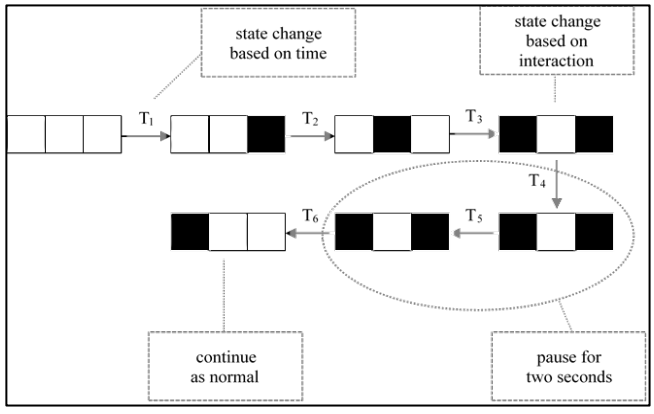

Fig 10. Simple Cellular Automata

2.5 Traffic Structure

After constructing cellular automata, the traffic model need to represent the road entity in the environment using set of cells. In other words, the model represents the continuous road in real-life by a discrete one. Therefore, when a vehicle

moves along the road, the displacement occur from one cell to another, progressively as illustrated in Figure 11.

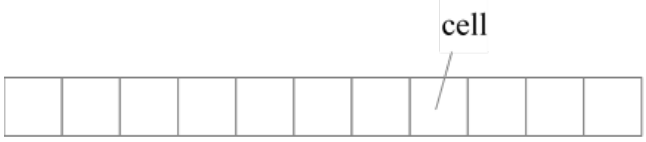

Fig 11. Representation of continuous road by discrete one (Cells) in Traffic Model

Similarly, it is important to measure a time in a discrete road. In discrete road passing of time is defined as a time step as shown in Figure 12. For the sake of consistency, a single time step is equivalent to a second. Although time can be measured in a smaller scale such as milliseconds etc., the smallest unit of time in the model is one second.

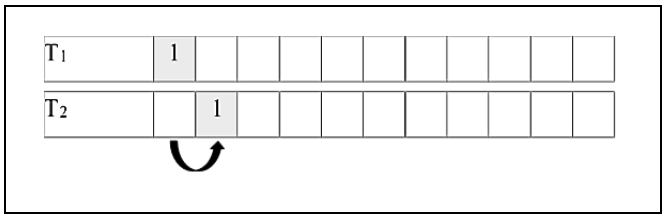

Fig 12. Time step

The velocity of the vehicle is defined as the cell velocity (v_{cell}) and abstracted into a range of discrete quantity. The most common range is between one to six or v = [0, 6]. The cell velocity signifies the number of cells that is traveled by the vehicle per time step or per second. Figure 13 illustrates the steps of determining the velocity based on the discrete time.

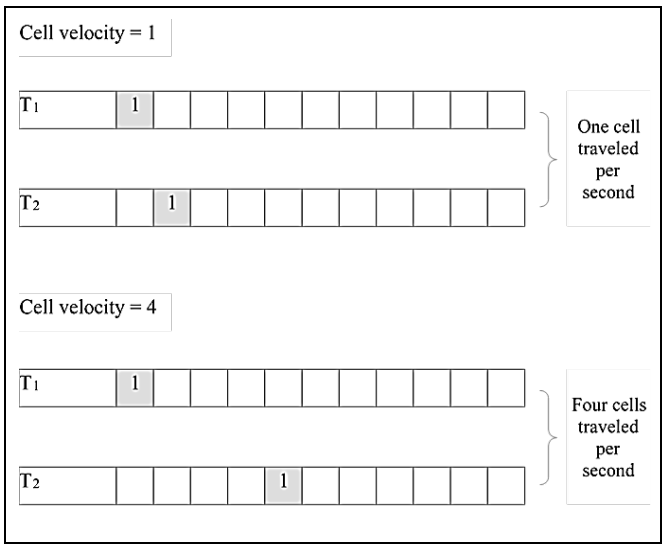

Fig 13. Graphical illustrates the steps of determining the velocity based on the discrete time.

When the cell velocity v_{cell} = 1 it is indicate that the vehicle is moving at one cell per second. In contrast, when the cell velocity v_{cell} = 4, the vehicle covers a total of four cells every second. If the maximum velocity of the vehicle in reality v_{max} is set at 120 km/h, then the velocity conversion between real velocity (v) and cell velocity (v_{cell}) can be derived by dividing the maximum real velocity with the maximum cell velocity ($v_{cellmax}$). Thus, the maximum real velocity is first converted into its equivalent m/s. The entire conversion between real velocity and cell velocity is given in Table 5. Each additional cell velocity contributes to 5.5555 m/s increase to the real velocity and vice-versa. Therefore, the real velocity = 5.5555m/s * cell velocity.

Table 5. Conversion of Real Velocity to Cell Velocity

Real Velocity		Cell Velocity
0 km/h	0.0000 m/s	0
20 km/h	5.5555 m/s	1
40 km/h	11.1111 m/s	2
60 km/h	16.6667 m/s	3
80 km/h	22.2222 m/s	4
100 km/h	27.7778 m/s	5
120 km/h	33.3333 m/s	6

In addition, the length of cell must be clearly defined when simulating the traffic. There are several traffic approaches can be taken, however, in this study the researcher considers the relationship between the real velocity and cell velocity. Hence, the cell velocity signifies the number of cells that a vehicle moves, within a time step or a second that is known from the conversion that each cell velocity translates to 5.5555 m/s to the real velocity. The length of each cell should be equivalent to 5.5555 m as demonstrated in the conversion of real length and cell length as in Figure 14.

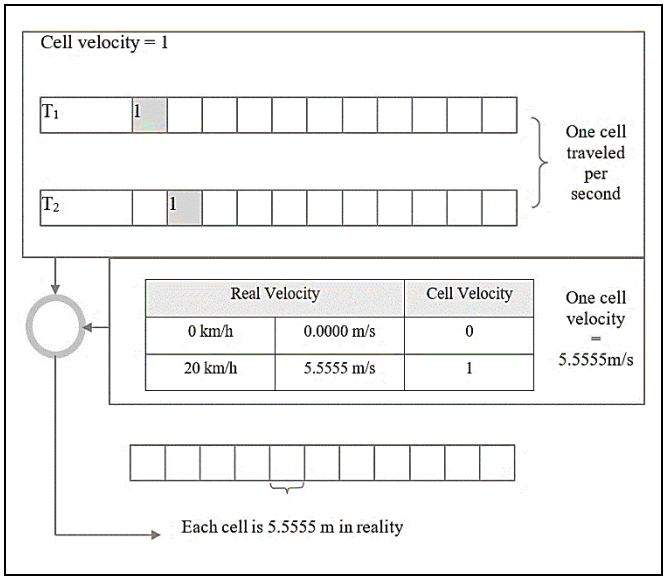

Fig 14. Conversion of Real Length and Cell Length

Figure 15 shows the controlled traffic flow through the arrival rate to illustrate clear scenario whereas Table 6 illustrated the simulated scenario. The scenario is divided into high, medium and low traffic flow where the environmental context is emphasized on a highway.

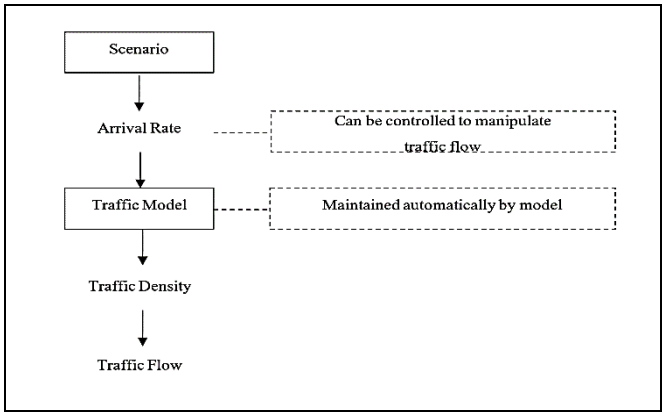

Fig 15. Controlled traffic flow through the arrival rate

Table Error! No text of specified style in document.**6.** Arrival Rate Scenario

No	Scenario	Arrival Rate	Arrival Rate
1 (High)	Peak hour e.g. 9am and 5pm when people are moving from their workplace and home	60	1.00
2 (Medium)	Non-peak hour e.g. during the day, such as 11am but excluding the peak hour period	40	0.67
3 (Low)	Early morning or in the middle of the night when most people are not on the Road	20	0.33

The arrival rate for the traffic behavior is modeled with the Poisson distribution. In effect, it can be mostly mediated by changing the arrival rate. Based on the traffic model, the maximum number of vehicles that can arrive on a single lane is 60 cars per minute or 1 car per second. Anything higher than that may cause a queue to the arrival where new vehicles cannot enter the initial cell of the traffic model until is it vacated. On the contrary, the minimum number of vehicles is set at 1 car per minute. For the case in the example, the high scenario is generated when the arrival rate is set at 60 vehicles per minute. Medium scenario where traffic flows semi-freely is defined at the arrival rate of 40 vehicles per minute. Finally, the low scenario where traffic flows freely is determined at the arrival rate of 20 vehicles per minute.

3. Results and Discussion

This section discusses and summarize the whole obtained results in terms of the total power generated for the tested arrival rates λ = 1.0, 0.5 and 0.1. To begin by the results of single lane and single piezoelectric, the results of this test shows that when the frequency of excitation increase the outputs power is also increased hence the Vehicles that move in real traffic may change their velocity and therefore, activate the piezoelectric device at different frequencies will affect the output power. In addition, the optimal resistance is between 200kΩ and 800kΩ. The model showed that power generation using the piezoelectric model was affected by the velocity and mass of the car which activated it. The vehicle velocity was based on the traffic flow in the model. This relationship was very fascinating. A higher traffic flow indicated that the vehicular movement was high during this period; however, it did not necessarily indicate the higher velocity of the piezoelectric activation. Hence, it has been considered the traffic flow at differing arrival rates. The traffic flow was considered when the mean arrival rate was set at the maximal value or λ =1. Based on the analysis, at high arrival rate, the traffic flow is 43.38 vehicle/minute. When the number of vehicles is high, the possibility of congestion is high as well. This may force the vehicles to lower their velocity to move in unison.

Considering the opposite scenario, when the arrival rate λ =0.1, which is the lowest value in the study, the traffic flow is considerably low. Here, it is only 5.98 vehicle/minute. Whereas the lowest outputs power is obtained at lower arrival rate and high resistance in the same figures. On the other hand, the results show that increase the resistance downgrade the obtained outputs power and decreases it smoothly until the outputs power reaches its lowest value.

The flow of traffic for three different mean arrival rates (λ) = 1.0, 0.5 and 0.1 are simulated via eight data sets for each case as detailed in Table 7.

Table 7. Flow of traffic for three different mean arrival rates

Data Set	Total Vehicle		
	λ = 1.0	λ = 0.5	λ = 0.1
1	7762.0	5064	1076
2	7846.0	5009	1065
3	7771.0	5018	1060
4	7853.0	5074	1077
5	7839.0	4993	1080
6	7777.0	5083	1089
7	7850.0	5111	1073
8	7774.0	5002	1090

The results also show that at low resistance the outputs power is always increase whenever the number of PCTs increase as well as the number of lanes increase. Table 4 summarizes the average of outputs power at arrival rate 1 and for different resistances with considering the number of lane and the number of PCTs.

Figure 16 showed an overview of the major aspects involved in the testing and evaluation of the model. Initially, the traffic flow was assessed for different arrival rates. Thereafter, the effect of resistance and mean arrival rate on the total generated power was analysed by crosshatching the set of resistances, ranging between 200-1600 kΩ.

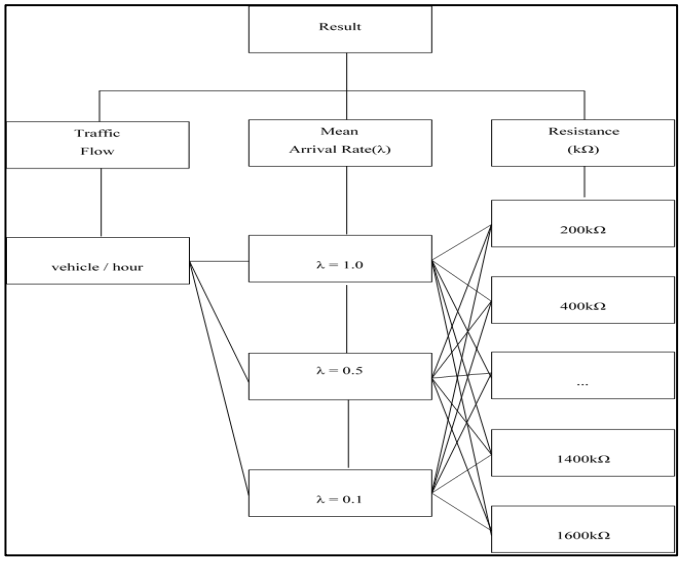

Fig 16. An overview on the most important aspects for simulation

*3.1 Testing single lane and one set array of 4*4 PCTs*

In this test, a single lane road and one set of PCTs array of size 4*4 were simulated. The results of this test are presented in Table 8 which presents the power against eight different resistance (kΩ) for three arrival rates (λ) = 1.0, 0.5 and 0.1. The results show that the obtained power is high when the resistance is low. This case is noted at three arrival rates. The results also show that the highest power could be obtained when the arrival rater is high.

Table 8. Average Power (W) vs Resistance (kΩ) for different Arrival Rate

Resistance (kΩ)	λ =1	λ =0.5	λ =0.1
	P1	P1	P1
200	86.146	63.208	13.908
400	92.908	76.220	15.946
600	85.376	68.425	18.905
800	73.201	60.361	16.574
1000	63.447	51.519	11.693
1200	55.746	46.529	10.282
1400	49.565	40.108	8.917
1600	44.284	36.302	7.781
P1 refer to Total Power when using one set array of 4*4 PCTs			

*3.2 Testing single lane and two set arrays of 4*4 PCTs*

In this test, a single lane road and two set of PCTs arrays of size 4*4 were simulated to harvest more power. The results of this test are presented in Table 9 and Table 10. The table presents the power (w) against eight different resistance (kΩ) for three arrival rates (λ) = 1.0, 0.5 and 0.1. Table 8 shows the average voltage for two lanes

Table 9. Average voltage (V) for two lanes vs Resistance (kΩ) for different Arrival Rate

Resistance (kΩ)	λ =1	λ =0.5	λ =0.1
	Av	Av	R1
200	144.16	177.44	166.55
400	223.21	272.68	252.13
600	272.21	313.54	290.11
800	295.65	334.60	310.37
1000	308.17	346.23	320.52
1200	314.46	353.08	326.04
1400	319.12	359.31	328.47
1600	325.24	363.10	332.47

Table 10. Total generated power (W) of single lane for different Arrival Rate

Resistance (kΩ)	λ =1	λ =0.5	λ =0.1
	Total	Total	Total
200	143.59	113.83	28.59
400	170.78	143.31	33.61
600	160.21	130.62	31.99
800	141.78	112.04	27.14
1000	123.78	101.64	23.53
1200	107.29	88.60	20.14
1400	96.66	77.45	17.83
1600	86.67	70.00	15.82
Total is the total generated power (W) of PCTs 1 and PCTs 2.			

The results also show that at low resistance the outputs power is always increase whenever the number of PCTs increase as well as the number of lanes increase. Table 11 summarizes the average of outputs power at arrival rate 1 and for eight resistances with considering the number of lane and the number of PCTs.

Table 11. Summary of the outputs power (W) at arrival rate 1 and for different resistances with considering the number of lane and the number of PCTs

Resistance kΩ)	Single lane		Two Lanes	
	1 PCTs array	2 PCTs arrays	1 PCTs array	2 PCTs arrays
200	86.146	143.59	127.03	286.96
400	92.908	170.78	148.61	345.25
600	85.376	160.21	141.72	319.03
800	73.201	141.78	121.63	277.41
1000	63.447	123.78	106.58	244.04
1200	55.746	107.29	91.68	215.53
1400	49.565	96.66	81.72	191.31
1600	44.284	86.67	74.22	175.73

Figure 17 represents the outputs power at arrival rates 1, 0.5 and 0.1 and when two lanes and two sets of PCTs arrays. The figure clearly summarizes that, the highest power is obtained at highest arrival rate and with low resistance 400 to 800 kΩ.

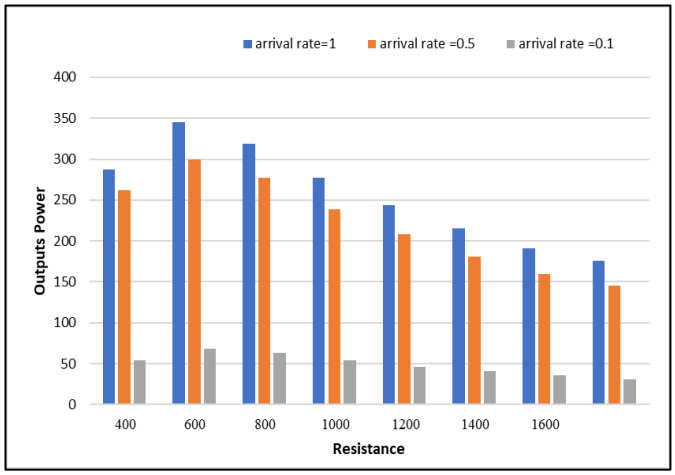

Fig 17. The power output at the arrival rate of 1, 0.5 and 0.1 when the model used 2 lanes and 2 sets of PCT arrays.

4. Conclusion

In conclusion, the results showed that for deriving the high output power, the model required a higher arrival rate and several PCTs. The total power was dependent on two factors. First, the velocity of which most vehicle passes through the piezoelectric device. Second, the total number of vehicles that activates the piezoelectric device within a duration which represents the arrival rate. In combination, the interplay of these two factors would determine the generation of total power at the piezoelectric entity. An amount of 345.25 W can be harvested at the highest mean arrival rate $\lambda = 1$. The traffic density in this case is very high in which many vehicles moving over the piezoelectric. When the mean arrival rate is lowest at $\lambda = 0.1$, the traffic flow is very low as well. Given that there are not many vehicles occupying the road. This ensures the maximization of the first factor.

Simulation of the model showed that the energy harvester could generate power using the piezoelectric traffic model in the 1-lane and 2-lane roads if the PCTs were implanted in arrays along the road. For harvesting a lot of power, the PCTs must be uniformly placed along the road. For a highway with a traffic volume of 600 vehicle/ h, and with the help of multiple PCT arrays, total electrical power of 170 kW/ km could be harvested. This harvested energy is used for powering the normal electric equipment on the roads like the lighting system, roadside advertisements and emergency communicating units.

5. Acknowledgement

The authors of this study acknowledge the financial support provided by the Ministry of Higher Education Malaysia, in the form of the ERGS research grant (Vote No. E035). They also wish to thank the Office for Research, Innovation, Commercialisation and Consultancy (ORICC) Management, UTHM for offering constant assistance and support in the management of the research grant.

Reference

[1]. Andriopoulou, S., *A review on energy harvesting from roads*. 2012.

[2]. Cook-Chennault, K., N. Thambi, and A. Sastry, *Powering MEMS portable devices—a review of non-regenerative and regenerative power supply systems with special emphasis on piezoelectric energy harvesting systems.* Smart Materials and Structures, 2008. **17**(4): p. 043001.

[3]. Hill, D., A. Agarwal, and N. Tong, *Assessment of Piezoelectric Materials for Roadway Energy Harvesting : Cost of Energy and Demonstration Roadmap*. 2014.

[4]. Kour, R. and A. Charif, *Piezoelectric roads: Energy harvesting method using piezoelectric technology.* Innov Ener Res, 2016. **5**(1).

[5]. Fry, D.N., D.E. Holcomb, J.K. Munro, L.C. Oakes, and M. Matson, *Compact portable electric power sources*. 1997, Oak Ridge National Lab., TN (United States).

[6]. Warneke, B., B. Atwood, and K.S. Pister. *Smart dust mote forerunners*. in *Micro Electro Mechanical Systems, 2001. MEMS 2001. The 14th IEEE International Conference on*. 2001. IEEE.

[7]. Widyawidura, W., M.N. Aridito, H.D. Kurniasari, and M. Kismurtono, *Waste-to-Energy Development Using Organic Waste Recycling System (OWRS): A Study Case of Giwangan Market.* International Journal of Renewable Energy Research (IJRER), 2019. **9**(1): p. 354-362.

[8]. Cheng, T.H., K.B. Ching, C. Uttraphan, and Y.M. Heong, *A Review on Energy Harvesting Potential from Living Plants: Future Energy Resource.* International Journal of Renewable Energy Research (IJRER), 2018. **8**(4): p. 2398-2414.

[9]. Colak, I., S. Sagiroglu, and M. Yesilbudak, *Data mining and wind power prediction: A literature review.* Renewable Energy, 2012. **46**: p. 241-247.

[10]. Soomro, D., S. Alswed, M. Omran, and U.H.O. Malaysia, *INVESTIGATION OFA SHUNT ACTIVE POWER FILTER WITH PI AND FUZZY LOGIC CONTROLLERS UNDER DIFFERENT LOADS.*

[11]. Roundy, S., E.S. Leland, J. Baker, E. Carleton, E. Reilly, E. Lai, B. Otis, J.M. Rabaey, P.K. Wright, and V. Sundararajan, *Improving power output for vibration-based energy scavengers.* IEEE Pervasive computing, 2005. **4**(1): p. 28-36.

[12]. Mitcheson, P.D., T.C. Green, E.M. Yeatman, and A.S. Holmes, *Architectures for vibration-driven micropower generators.* Journal of microelectromechanical systems, 2004. **13**(3): p. 429-440.

[13]. MIYAZAKI, M., H. TANAKA, G. ONO, T. NAGANO, N. OHKUBO, and T. KAWAHARA, *Electric-energy generation through variable-capacitive resonator for power-free LSI.* IEICE Transactions on Electronics, 2004. **87**(4): p. 549-555.

[14]. Torah, R., S. Beeby, M. Tudor, T. O'Donnell, and S. Roy, *Development of a Cantilever Beam Generator Employing Vibration Energy Harvestin.* 2006.

[15]. Roundy, S., P.K. Wright, and J. Rabaey, *A study of low level vibrations as a power source for wireless sensor nodes.* Computer communications, 2003. **26**(11): p. 1131-1144.

[16]. Bottner, H., J. Nurnus, A. Gavrikov, G. Kuhner, M. Jagle, C. Kunzel, D. Eberhard, G. Plescher, A. Schubert, and K.-H. Schlereth, *New thermoelectric components using microsystem technologies*. Journal of microelectromechanical systems, 2004. **13**(3): p. 414-420.

[17]. Moheimani, S.R. and A.J. Fleming, *Piezoelectric transducers for vibration control and damping*. 2006: Springer Science & Business Media.

[18]. Liu, H., J. Zhong, C. Lee, S.-W. Lee, and L. Lin, *A comprehensive review on piezoelectric energy harvesting technology: Materials, mechanisms, and applications.* Applied Physics Reviews, 2018. **5**(4): p. 041306.

[19]. Eichhorn, C., R. Tchagsim, N. Wilhelm, and P. Woias, *A smart and self-sufficient frequency tunable vibration energy harvester.* Journal of Micromechanics and Microengineering, 2011. **21**(10): p. 104003.

[20]. Williams, C. and R.B. Yates, *Analysis of a micro-electric generator for microsystems*. sensors and actuators A: Physical, 1996. **52**(1): p. 8-11.

[21]. Zhang, Z., H. Xiang, and Z. Shi, *Modeling on piezoelectric energy harvesting from pavements under traffic loads.* Journal of Intelligent Material Systems and Structures, 2015: p. 1045389X15575081.

[22]. Rhimi, M. and N. Lajnef, *Tunable energy harvesting from ambient vibrations in civil structures.* Journal of Energy Engineering, 2012. **138**(4): p. 185-193.

[23]. Peigney, M. and D. Siegert, *Piezoelectric energy harvesting from traffic-induced bridge vibrations.* Smart Materials and Structures, 2013. **22**(9): p. 095019.

[24]. Choi, W., Y. Jeon, J.-H. Jeong, R. Sood, and S.-G. Kim, *Energy harvesting MEMS device based on thin film piezoelectric cantilevers.* Journal of Electroceramics, 2006. **17**(2-4): p. 543-548.

[25]. Jeon, Y., R. Sood, J.-H. Jeong, and S.-G. Kim, *MEMS power generator with transverse mode thin film PZT.* Sensors and Actuators A: Physical, 2005. **122**(1): p. 16-22.

[26]. Chua, H.G., B.C. Kok, and H.H. Goh, *Modelling And Design Analyses Of A Piezoelectric Cymbal Transducer (PCT) Structure For Energy Harvesting Application.* Energy and Sustainability V, 2014. **186**: p. 103.

[27]. Zhao, H., J. Ling, and J. Yu, *A comparative analysis of piezoelectric transducers for harvesting energy from asphalt pavement*. Journal of the Ceramic Society of Japan, 2012. **120**(1404): p. 317-323.

[28]. Li, X., M. Guo, and S. Dong, *A flex-compressive-mode piezoelectric transducer for mechanical vibration/strain energy harvesting.* IEEE transactions on ultrasonics, ferroelectrics, and frequency control, 2011. **58**(4): p. 698-703.

[29]. Gareh, S., B. Kok, C. Uttraphan, K. Thong, and A. Borhana. *Evaluation of piezoelectric energy harvester outcomes in road traffic applications*. in *4th IET Clean Energy and Technology Conference (CEAT 2016)*. 2016. IET.

[30]. Thong, K.T., B. Kok, C. Uttraphan, S. Gareh, and Z.J. Sam. *Data acquisition system for Piezoelectric Cymbal Transducer energy harvesting*. in *2016 IEEE International Conference on Power and Energy (PECon)*. 2016. IEEE.

[31]. Viola, F., P. Romano, R. Miceli, and G. Acciari. *On the harvest of rainfall energy by means of piezoelectric transducer*. in *2013 International Conference on Renewable Energy Research and Applications (ICRERA)*. 2013. IEEE.

[32]. Verbelen, Y. and A. Touhafi. *Resource considerations for durable large scale renewable energy harvesting applications*. in *2013 International Conference on Renewable Energy Research and Applications (ICRERA)*. 2013. IEEE.

[33]. Tourou, P., J. Chhor, K. Günther, and C. Sourkounis. *Energy storage integration in DFIG-based wind energy conversion systems for improved fault ride-through capability*. in *2017 IEEE 6th International Conference on Renewable Energy Research and Applications (ICRERA)*. 2017. IEEE.

[34]. Minami, M., T. Sakabe, S.-i. Motegi, and M. Michihira. *An Experimental Verification for Improvement of Output Characteristics by LC Resonance in Vibration Generators with Boost-type Current-Improving Passive Rectifier*. in *2018 7th International Conference on Renewable Energy Research and Applications (ICRERA)*. 2018. IEEE.

[35]. Özdemır, A.E. and S.A. Oy. *Alternative renewable energy producing systems by utilizing piezoelectric transducers*. in *Renewable Energy Research and Applications (ICRERA), 2016 IEEE International Conference on*. 2016. IEEE.

[36]. Alswed, S.K., *Improved droop control for parallel inverter system with load*. 2014.

[37]. Tominaga, Y., M. Tanaka, H. Eto, Y. Mizuno, N. Matsui, and F. Kurokawa. *Design Optimization of Renewable Energy System Using EMO*. in *2018 International Conference on Smart Grid (icSmartGrid)*. 2018. IEEE.

[38]. Zafar, B., *Design of a Renewable hybrid photovoltaic-Electrolyze-PEM/Fuel Cell System using Hydrogen Gas.* International Journal of Smart Grid-ijSmartGrid, 2019. **3**(4): p. 201-207.

[39]. Jiang, X., Y. Li, J. Wang, and J. Li, *Electromechanical modeling and experimental analysis of a compression-based piezoelectric vibration energy harvester.* International Journal of Smart and Nano Materials, 2014. **5**(3): p. 152-168.

[40]. Jiang, X., Y. Li, J. Li, J. Wang, and J. Yao, *Piezoelectric energy harvesting from traffic-induced pavement vibrations.* Journal of Renewable and Sustainable Energy, 2014. **6**(4): p. 043110.

[41]. Gareh, S., B. Kok, M. Yee, A.A. Borhana, and S. Alswed, *Optimization of the Compression-Based Piezoelectric Traffic Model (CPTM) for Road Energy Harvesting Application.* International Journal of Renewable Energy Research (IJRER), 2019. **9**(3): p. 1272-1282.

[42]. Nagel, K. and M. Schreckenberg, *A cellular automaton model for freeway traffic*. Journal de physique I, 1992. **2**(12): p. 2221-2229.

[43]. Safaei, M., H.A. Sodano, and S.R. Anton, *A review of energy harvesting using piezoelectric materials: State-of-the-art a decade later (2008-2018)*. Smart Materials and Structures, 2019.

[44]. Kok, B., S. Gareh, H. Goh, and C. Uttraphan. *Electromechanical-Traffic Model of Compression-Based Piezoelectric Energy Harvesting*. in *MATEC Web of Conferences*. 2016. EDP Sciences.

[45]. Kwok, K., T. Lee, S. Choy, and H. Chan, *Lead-free piezoelectric transducers for microelectronic wirebonding applications.* Piezoelectric Ceramics, 2010. **3**: p. 145-64.

[46]. Bain, N., T. Emig, F.-J. Ulm, and M. Schreckenberg, *Velocity statistics of the Nagel-Schreckenberg model.* Physical Review E, 2016. **93**(2): p. 022305.

[47]. Guidolin, M., A.S. Chen, B. Ghimire, E.C. Keedwell, S. Djordjević, and D.A. Savić, *A weighted cellular automata 2D inundation model for rapid flood analysis.* Environmental Modelling & Software, 2016. **84**: p. 378-394.

[48]. Jazar, R.N., *Vehicle dynamics: theory and application*. 2013: Springer Science & Business Media.